Ulrike Hess, Shakiba Shahabi, Laura Treccani, Philipp Streckbein, Christian Heiss, Kurosch Rezwan

Co-delivery of cisplatin and doxorubicin from calcium phosphate beads/matrix scaffolds for osteosarcoma therapy

Journal Article as: peer-reviewed accepted version (Postprint)

DOI of this document*(secondary publication): 10.26092/elib/2621

Publication date of this document: 03/11/2023

* for better findability or for reliable citation

Recommended Citation (primary publication/Version of Record) incl. DOI:

Ulrike Hess, Shakiba Shahabi, Laura Treccani, Philipp Streckbein, Christian Heiss, Kurosch Rezwan,
Co-delivery of cisplatin and doxorubicin from calcium phosphate beads/matrix scaffolds for osteosarcoma therapy,
Materials Science and Engineering: C, Volume 77, 2017, Pages 427-435, ISSN 0928-4931,
https://doi.org/10.1016/j.msec.2017.03.164

Co-delivery of cisplatin and doxorubicin from calcium phosphate beads/matrix scaffolds for osteosarcoma therapy

Ulrike Hess [a], Shakiba Shahabi [a], Laura Treccani [a,*,1], Philipp Streckbein [b,d], Christian Heiss [c,d], Kurosch Rezwan [a,e]

[a] Advanced Ceramics, University of Bremen, Am Biologischen Garten 2, 28359 Bremen, Germany
[b] Department for Cranio-Maxillofacial and Plastic Surgery, University Hospital of Giessen-Marburg GmbH, Campus Giessen, Klinikstrasse 33, 35392 Giessen, Germany
[c] Department of Trauma, Hand and Reconstructive Surgery, University Hospital of Giessen-Marburg GmbH, Campus Giessen, Rudolf-Buchheim-Strasse 7, 35392 Giessen, Germany
[d] Laboratory of Experimental Surgery, Justus-Liebig-University of Giessen, Kerkrader Strasse 9, 35394 Giessen, Germany
[e] MAPEX Center for Materials and Processes, University of Bremen, Am Fallturm 1, 28359 Bremen, Germany

Keywords:
Co-delivery
Scaffold
Drug carrier
Doxorubicin
Cisplatin

A B S T R A C T

Bone substitute materials with a controlled drug release ability can fill cavities caused by the resection of bone tumours and thereby combat any leftover bone cancer cells. The combined release of different cytostatics seems to enhance their toxicity. In this study, calcium phosphate beads and matrix scaffolds are combined for a long-term co-delivery of *cis*-diamminedichloroplatinum (cisplatin, CDDP) and doxorubicin hydrochloride (DOX) as clinical relevant model drugs. Tricalcium phosphate/alginate beads as additional drug carrier are produced by droplet extrusion with ionotropic gelation and incorporated in scaffold matrix by freeze gelation without sintering. CDDP shows a short burst release while DOX has a continuous release measurable over the entire study period of 40 days. Drug release from matrix is decreased by ~30% compared to release from beads. Nevertheless, all formulations follow the Korsmeyer-Peppas release kinetic model and show Fickian diffusion. Cytotoxic activity was conducted on MG-63 osteosarcoma cells after 1, 4, and 7 days with WST-1 cell viability assay. Co-loaded composites enhance activity towards MG-63 cells up to ~75% toxicity while reducing the released drug quantity. The results suggest that co-loaded beads/matrix scaffolds are highly promising for osteosarcoma therapy due to synergistic effects over a long period of more than a month.

1. Introduction

Despite improved surgical, radio, and chemotherapeutic techniques, bone cancer still is one of the major causes of severe functional and structural skeletal defects or even death. A major risk for pathologic fractures, severe pain, life-threatening hypercalcaemia, and an overall increased mortality is the local recurrence by residual neoplastic cells remaining due to incomplete marginal resection [1–3].

To control or prevent the risk of local recurrence of bone cancer, local administration by drug carriers can deliver cytostatics in high concentrations with enhanced efficacy to the tumour while minimizing the drug concentrations in the bloodstream or other organs and improving the patient comfort. These carriers include hydrogels [4,5], micro- and nano-particles [5–7], liposomes [8], biodegradable polymers [9,10], or calcium phosphates [6,11]. However, degrading fragments or acidic byproducts, from biodegradable polymer-based drug delivery systems or harsh solvents required for their degradation may adversely affect the drugs to be delivered or the surrounding tissues [12]. For polymer-based systems, often an undesired massive and uncontrolled late stage drug release was observed [13].

In contrast, drug release from calcium phosphates (CaP), usually driven by desorption, is more evenly and can be better controlled [12]. CaP has excellent biocompatibility, bioactivity, and osteoconductivity due to its chemical and physical resemblance to bone mineral [14,15]. Especially apatites has high surface interaction properties and can bind neutral, positively, and negatively charged molecules enabling a delivery of a wide range of pharmaceuticals such as anticancer drugs [12,16]. The localized drug release from CaP-based drug delivery systems can result in tumour inhibition and can minimize high systemic drug concentration to much lower, less-toxic systemic values and can thereby reduce the need for repeated dosing making it more

* Corresponding author at: Petroceramics SpA c/o Kilometro Rosso Science & Technology Park, Viale Europa 2, 24040 Stezzano, BG, Italy.
E-mail addresses: uhess@uni-bremen.de (U. Hess), shahabi@uni-bremen.de (S. Shahabi), treccanilaura@gmail.com, treccani@petroceramics.com (L. Treccani), philipp.streckbein@uniklinikum-giessen.de (P. Streckbein), christian.heiss@chiru.med.uni-giessen.de (C. Heiss), krezwan@uni-bremen.de (K. Rezwan).
[1] Present address: Petroceramics SpA c/o Kilometro Rosso Science & Technology Park, Viale Europa 2, 24040 Stezzano, BG, Italy.

comfortable for the patient [12,16]. Consequently, CaP ceramic is an ideal candidate for the dual role as principal filling material for bone defects and for drug-carrying.

In this study we present a CaP beads/matrix composite as open-porous, resorbable scaffold co-loaded for osteosarcoma therapy with two model but clinically relevant cytostatics, namely *cis*-diamminedichloroplatinum (cisplatin, CDDP, *cis*-[$PtCl_2(NH_3)_2$]) [17,18] and doxorubicin hydrochloride (DOX, $C_{27}H_{29}NO_{11}\cdot HCl$) [19]. While the toxicity of CDDP is based on binding to DNA which leads to apoptosis [20,21], DOX is an anthracycline antibiotic which prevents cell replication by intercalating in DNA [22].

Combination chemotherapy using two or more drugs has been proven to be effective and clinically successful [23,24]. Using several drugs can enhance the overall cytotoxicity of each drug at reduced doses, maximizing therapeutic efficacy and overcoming drug resistance [8,25]. The multicomponent drug treatment may lead to additive, synergistic, or antagonistic effects. This applies also to the combination of CDDP and DOX which may yield strong synergy in the efficacy and may show an increased response rate [26,27].

β-Tricalcium phosphate beads were prepared by droplet extrusion coupled with ionotropic gelation, an established method to produce ceramic beads with tuneable properties [28,29]. They were incorporated in a hydroxyapatite matrix scaffold fabricated via freeze gelation. The possibility to employ these scaffolds as cytostatic depot either by loading matrix and/or beads on cytostatic release was assessed and toxicity of released solutions was evaluated via WST-1 assay on MG-63 osteosarcoma cells.

2. Materials and methods

2.1. Materials

β-Tricalcium phosphate (TCP, specific surface area of 1.1 m^2/g, lot. BCBB7609) powder, hydroxyapatite (HAP, specific surface area of 65 m^2/g, lot. A3420) powder, anhydrous citric acid (lot. BCBB7128), concentrated ammonium hydroxide solution (≥25%, lot. SZBA1400), tris(hydroxymethyl)aminomethane (Tris, lot. MKBD9221V), *n*,*n*-dimethylformamide (DMF, biotech. grade ≥ 99.9%, lot. SHBD8911V), *o*-phenylenediamine (peroxidase substrate ≥ 98.0%, lot. SLBC9002V), 0.1 M sodium phosphate monobasic monohydrate (ACS reagent, 98.0–102.0%, lot. BCBG8983V), 0.1 M sodium phosphate dibasic (≥99%, cell culture tested, lot. BCBD8825V), foetal calf serum (FCS, lot. 010M3395), and *cis*-diamineplatinum(II)dichloride (cisplatin, CDDP, ≥ 99.9%, trace metals basis, lot. MKBR7630V) were purchased from Sigma-Aldrich (Germany). Calcium chloride dihydrate (lot. BCBK7809V) and hydrochloric acid solution (1 M, lot. SZBB2900V) were supplied from Fluka (Germany). Doxorubicin hydrochloride CRS (DOX, code D2975000, batch 6.1, European Pharmacopoeia Reference Standard, France), tri-sodium citrate dihydrate (1 M, lot. 3Z003926, AppliChem, Germany), Dulbecco/Vogt modified Eagle's minimal essential medium (DMEM, high glucose, lot. 1206393, Invitrogen, Germany), antibiotic-antimycotic (lot. 1209917, Invitrogen, Germany), sodium alginate (viscosity of 350–550 mPas, lot. 9O008361, BioChemica, Germany), ammonia stabilised silica sol (SiO_2 content of 30 vol%, particle size of 5–8 nm, surface area of 230–360 m^2/g, BINDZIL® 30NH3/220, lot. 0590b, Eka Chemicals, Germany), and absolute ethanol (≥99.8%, lot. 14G080506, VWR, France) were obtained from different suppliers as specified and used without further purification. Cell culture tests were carried with human osteosarcoma cells (MG-63, passage 98, lot. 2006399, ATCC, Germany). Double deionised water (ddH_2O) with a conductivity of 0.05 μS/cm obtained from an ultra-pure water system (Synergy system, Millipore, Germany) was used for all studies.

2.2. Bead preparation

TCP beads were obtained by ionotropic gelation via droplet extrusion using a protocol adapted from Klein et al. [28]. Briefly, a TCP/alginate suspension was prepared by adding TCP (15.4 wt%) stepwise under stirring (1000 r/min, Dispermat LC-2, VMA-Getzmann, Germany) to a water-based suspension containing sodium alginate (0.7 wt%), silica sol (30.3 wt%) and sodium citrate (0.2 wt%) (Fig. 1). To remove possible agglomerates, the suspension was homogenized for 15 min with an ultrasound horn (Sonifier 450, Branson, Germany; power: 150 W, pulse rate: 0.5 s). Subsequently, the suspension was dropped with a syringe (5 ml Injekt® Luer Solo; needle diameter: 0.55 mm) in a cross-linking solution of ddH_2O and ethanol (ddH_2O/ethanol ratio: 80/20 v/v) and 0.1 mol/l calcium chloride. Beads were left in the cross-linking solution at room temperature for 18 h. Afterwards they were washed three times with ddH_2O to remove excessive calcium ions from their surface. The beads were frozen for 30 min at −150 °C (Ultra-Low Temperature Freezer MDF-1155, Sanyo Electric Biomedical, Japan) and subsequently freeze dried at −20 °C (P8K-E-80-4-80 °C, Piatkowski, Germany) for ~5 days. The beads were used without any further treatment or sintering.

2.3. Bead loading

For loading the TCP beads with cytostatics, concentrated solutions with 60 μg/ml CDDP or 60 μg/ml DOX (Fig. 2,B) dissolved in ddH_2O were used (Fig. 1). 0.5 ml cytostatic stock solution was added to 0.055 g beads and incubated at 37 °C under continuous shaking at 100 r/min (Unimax 1010 with Inkubator 1000, Heidolph Instruments, Germany) to guarantee a uniform drug load. After DOX and CDDP supernatants were removed after 60 min and 48 h, respectively, they were centrifuged for 15 min at 14500 r/min (Heraeus Fresco 21, Thermo Scientific, Germany) to separate and remove any particulates.

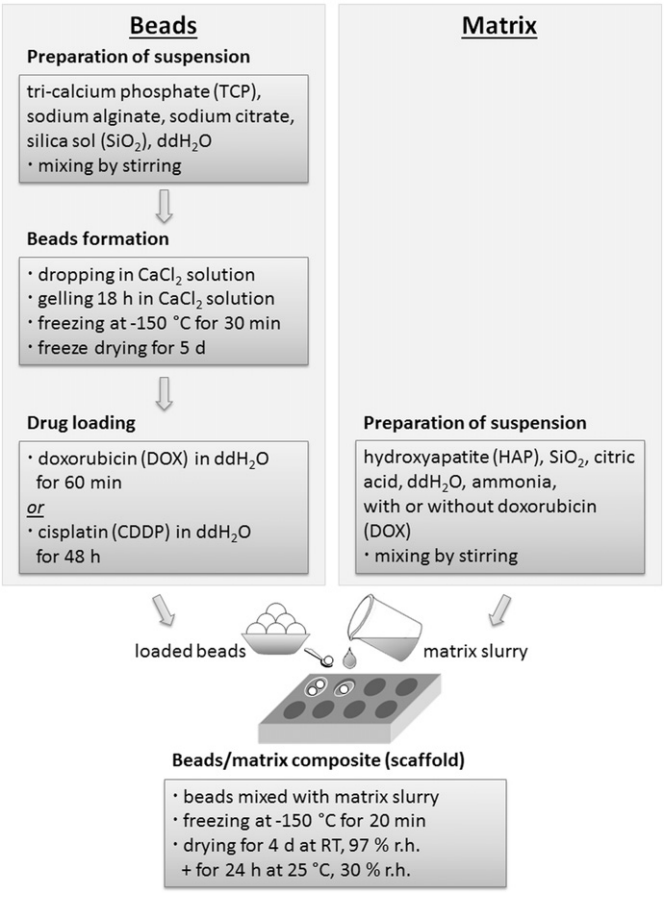

Fig. 1. Schematic representation of non-sintered tricalcium phosphate (TCP) beads production, drug loading and beads/matrix composite preparation.

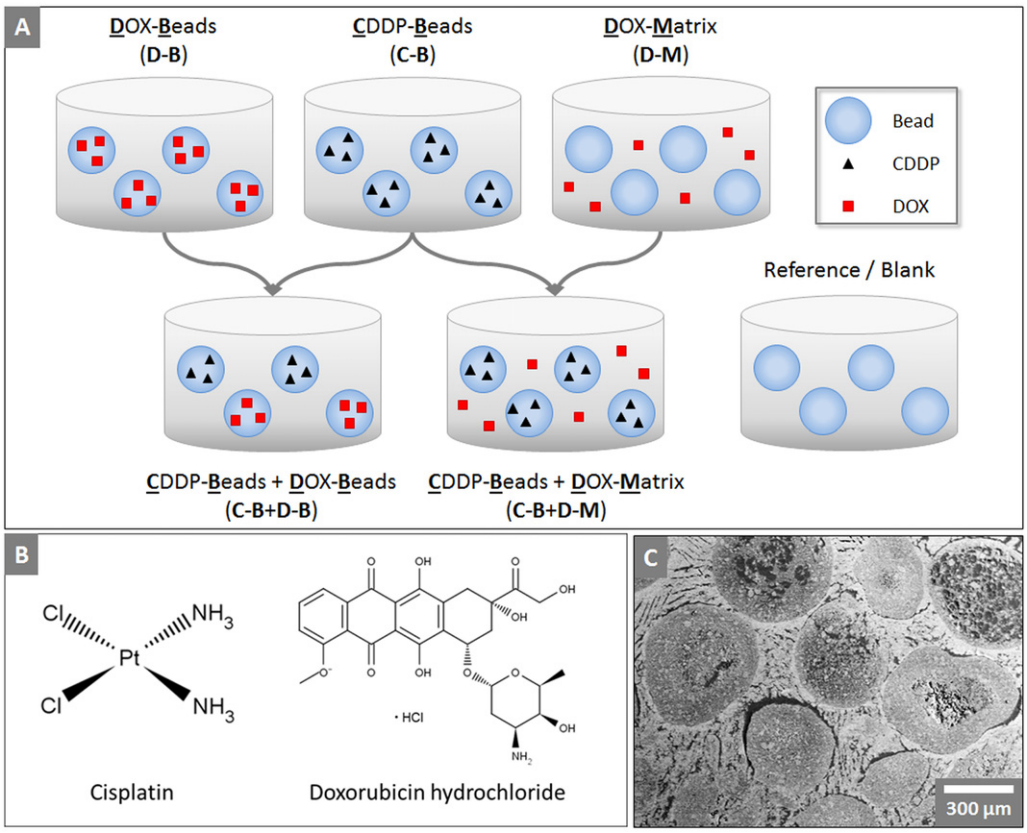

Fig. 2. A: Schematic of the five different types of beads/matrix composite scaffolds considered in this study. Beads loaded with cisplatin (CDDP) and/or doxorubicin (DOX) or non-loaded beads were used. For two sample types additionally the matrix was loaded with DOX. For all investigations non-loaded beads/matrix composites were used as reference. B: Molecular structure of cisplatin (CDDP) and doxorubicin hydrochloride (DOX). C: SEM image showing the cross section of a porous bead/matrix composite.

The amount of loaded DOX was spectroscopically measured over 90 min. Kinetic measurements were carried out by adding 1 ml DOX solution (30 µg/ml) to 0.055 g TCP beads in a semi-micro cuvette (UV-Cuvette semi-micro, Brand, Germany). DOX concentration in the supernatant was directly measured at 480 nm (Multiskan GO, Thermo Scientific, Finland) every 2 min. Between two measuring time points the beads were mixed to obtain a uniform drug loading. The amount of loaded DOX was calculated by subtracting of the absorbance value of DOX in the supernatant from the absorbance value of the stock solution.

The amount of CDDP in supernatant was determined via a derivatization reaction using a modified protocol from [30,31]. 100 µl supernatant was mixed with 100 µl *o*-phenylenediamine (OPDA) solution (1.4 mg/ml in DMF) and 200 µl phosphate buffer pH 6.8, in this order. The mixture was heated at 100 °C for 10 min (ThermoMixer® C, Eppendorf, Germany) till the solution turned light blue. After cooling to room temperature, the solution was filled with DMF up to 1 ml and the absorbance was measured at $\lambda_{max} = 705$ nm using a UV/VIS spectrophotometer. For both drugs, measurements were done in quadruplicates.

2.4. Composite preparation

For beads/matrix composites, TCP beads were incorporated in an open-porous HAP matrix obtained by freeze gelation as described in our previous studies [32–34]. Shortly, a homogenous water-based suspension consisting of HAP (59.34 wt%), silica sol (1.98 wt%), citric acid (1.93 wt%) and with a final pH of 8 was first prepared. Different composites were obtained by either adding DOX to the matrix suspension or DOX and CDDP loaded beads were incorporated into the matrix. Five different sample types were produced and evaluated and details about beads/matrix composites composition are given in Fig. 2,A and Table 1. To incorporate DOX in the HAP matrix, 30 µg/composite (~0.0023 wt% DOX) were added to the suspension. It is worth to note that it was not possible to load CDDP in the matrix due to its very limited

Table 1
Composition of the beads/matrix composite scaffolds with respect to drug loading. (– = not included) (mean ± SD).

Formulation	Beads amount in composite (g) and (wt%)			Loaded drug amount (µg/composite)		
	Beads unloaded	Beads with CDDP	Beads with DOX	CDDP in beads	DOX in beads	DOX in matrix
DOX in **B**eads (D-B)	0.055 ± 0.001 (4.3)	–	0.055 ± 0.001 (4.3)	–	29.28 ± 0.63	–
CDDP in **B**eads (C-B)	0.055 ± 0.001 (4.3)	0.055 ± 0.001 (4.3)	–	29.03 ± 0.33	–	–
DOX in **M**atrix (D-M)	0.110 ± 0.002 (8.6)	–	–	–	–	30 ± 0.26
CDDP in **B**eads + **D**OX in **B**eads (C-B + D-B)	–	0.055 ± 0.001 (4.3)	0.055 ± 0.001 (4.3)	29.03 ± 0.33	29.28 ± 0.63	–
CDDP in **B**eads + **D**OX in **M**atrix (C-B + D-M)	0.055 ± 0.001 (4.3)	0.055 ± 0.001 (4.3)	–	29.03 ± 0.33	–	30 ± 0.26

solubility in aqueous solutions [35]. Non-loaded composites were used as reference for release tests and cytotoxicity analysis.

Beads were incorporated in the HAP matrix by mixing beads in the HAP suspension. For each sample 0.11 g beads were used and they correspond to 8.6 wt%. The beads/matrix suspension was then homogenously distributed in cylindrical polyvinyl chloride (PVC) moulds (diameter: 10 mm; height: 5 mm). The moulds were frozen for 20 min at −150 °C. Demoulded specimens were dried at room temperature and a relative humidity (r.h.) of ~97% for 4 days in a desiccator and finally dried an additional day at 25 °C and 30% r.h.

2.5. Bead and composite characterisation

The density of beads and composite was measured by helium-pycnometrie (Pycomatic ATC, Thermo Scientific, Italy). Specific surface area (S_{BET}) as well as beads pore volume were determined by nitrogen adsorption (Belsorp-Mini, Bel, Japan) using the Brunauer-Emmett-Teller (BET) method [36]. Beads and composite open porosity and pore sizes were measured via mercury-intrusion porosimetry (Pascal 140/440, Porotec, Germany). Contact angle and surface tension of mercury were assumed to be 141.3° and 480 mN/m, respectively. Total porosity of composites was calculated by considering the final specimen size, weight and density. Beads and scaffolds were imaged via scanning electron microscopy (SEM, acceleration voltage 20 kV, CamScan, UK) after they were sputtered with a thin gold layer (Emitech K550, Judges Scientific, UK).

2.6. Drug release

DOX and CDDP release from beads/matrix scaffold composites was monitored over a period of 40 days in 1 ml Tris-HCl buffer (0.1 mol/l, initial pH of 7.4) at 37 °C and under continuous shaking. At each measuring time point, Tris-HCl was completely removed and replaced with an equivalent amount of fresh Tris-HCl. The initial cytostatic release was determined after 7, 31 and 55 h of exposure and then every 1 day. Non-loaded beads/matrix composites were used as reference.

Table 2
Properties of non-sintered β-tricalcium phosphate (TCP) beads (mean ± SD).

Characteristic	Value
Density ρ (g/cm^3)[†]	2.54 ± 0.001
Diameter d (mm)[$]	0.96 ± 0.27
Specific surface area S_{BET} (m^2/g)[‡]	55.8 ± 0.4
Open porosity Φ (%)[§]	50.5 ± 3.3
Pore volume V_P (mm^3/g)[‡]	45.5 ± 6.3
Average pore diameter d_P (nm)[§]	20/122
Pore size distribution[§]	Bimodal

Measured by: He-pycnometry[†], geometrical measurement[$], N_2-adsorption[‡], Hg-intrusion[§].

Measurement was done in triplicate and all samples were used in quadruplicates.

The released DOX quantity in supernatants was measured directly by fluorescence spectrometry (Plate CHAMELEON™V Multilabel Microplate Reader, Hidex, Finland) with an excitation wavelength at λ_{ex} = 485 nm and an emission wavelength at λ_{em} = 590 nm.

The released CDDP quantity in Tris-HCl buffer could not be measured by derivatization with OPDA due to interactions between the derivatisation reagent and buffer components. Instead, released CDDP quantity was determined by multi-component analysis and Bert-Lambert law [37].

2.7. Release kinetic

To evaluate the drug release mechanisms and kinetics four different models were used to fit the results of the in vitro release data. As kinetic models zero-order kinetic (cumulative percentage drug released vs. time), first-order kinetic (log cumulative percentage of drug remaining vs. time), Higuchi's model (cumulative percentage drug released vs. square root of time) and Korsmeyer-Peppas model (log cumulative percentage drug released vs. log time) were used [38–41]. From the linear regression of these plots the correlation coefficient (R^2) values were calculated and compared.

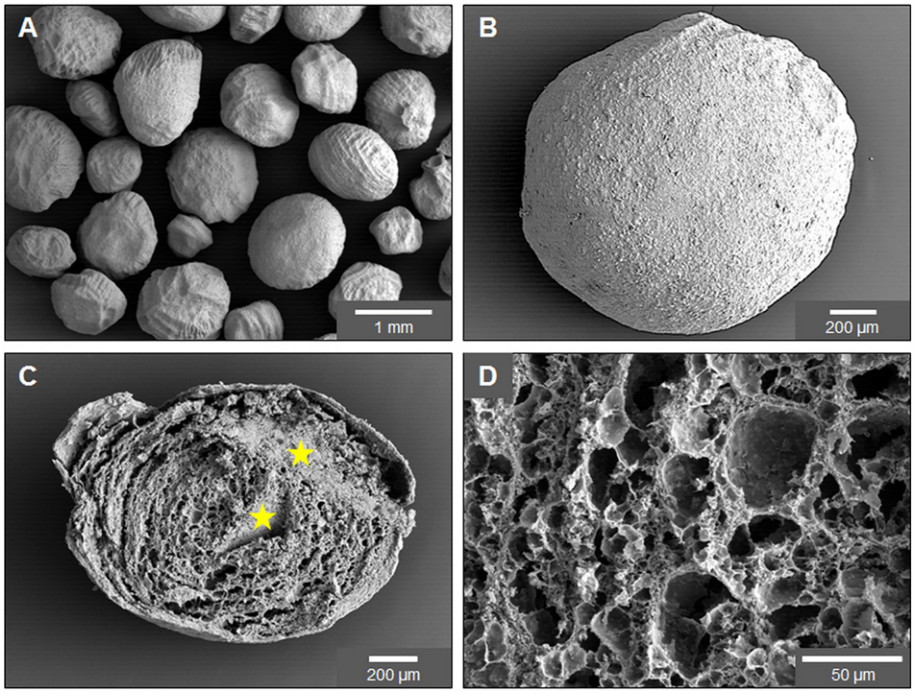

Fig. 3. SEM micrographs of non-sintered β-tricalcium phosphate (TCP) beads (A), bead surface (B), bead cross section (C), and detail of the porous inner bead structure (D). (⋆: densified area due to sectioning).

The equations for the different release kinetic models were as follows:

- Zero-order kinetic:

$$Q_t = Q_0 + K_0 t \quad (1)$$

- First-order kinetic:

$$\ln Q_t = \ln Q_0 + K_1 t \quad (2)$$

- Higuchi's model:

$$Q_t = K_H \sqrt{t} \quad (3)$$

- Korsmeyer-Peppas model:

$$M_t/M_\infty = kt^n \quad (4)$$

where Q_0 is the initial amount of drug in solution (it is usually zero), Q_t is the amount of drug released in time t, K_0 is the zero-order release constant, K_1 is the first-order release constant, K_H is the Higuchi dissolution constant, M_t/M_∞ is the fraction of drug released at time t, k is the rate constant, and n is the release exponent of the Korsmeyer-Peppas model.

The interpretation of the diffusional constant n for a cylindrically shaped sample was done according to [41–43]:

- $n \leq 0.45$ Fickian diffusion
- $0.45 < n < 0.89$ Anomalous (non-Fickian) transport
- $n = 0.89$ Case-II transport
- $n > 0.89$ Super case-II transport

2.8. Cell viability

2.8.1. Cell culture

In vitro cell viability was assessed with osteosarcoma cell line MG-63 (passage 98, lot. 2006399, ATCC, Germany). Briefly, the cells were cultured in DMEM (Dulbecco/Vogt modified Eagle's minimal essential medium) supplemented with 10% heat-inactivated FCS (foetal calf serum) and 1% antibiotic-antimycotic in a cell incubator (C200, Labotect Labor-Technik-Göttingen GmbH, Germany) at standard conditions (37 °C, 9.3% CO_2, 95% r.h.). All three (DMEM, FCS, antibiotic-antimycotic) together is hereinafter referred to as cell medium. For up to 1 week, cells were cultured in cell culture flasks (75 cm^2, NUNC, Fischer Scientific, Germany) and the cell medium was refreshed every 2 days [44–47].

2.8.2. Sample collection

To determine cell viability, using a modified protocol from [48,49]. First, beads/matrix composites were soaked in 2 ml Tris-HCl buffer at 37 °C, under continuous shaking at 100 r/min for 1, 4, and 7 days and without changing the buffer. Media containing the released drugs were removed and centrifuged for 15 min at 14500 r/min to remove possible particulates. Media were diluted with cell medium (ratio extraction medium/cell medium: 1/9) and then added to wells with MG-63 cells.

2.8.3. Cell viability

Cells were seeded at an initial density of 2.5×10^4 cells/ml medium onto Thermanox® coverslips (Ø = 15 mm, NUNC, Fischer Scientific, Germany) placed in wells of a 24-well polystyrene multidish (NUNC, Fischer Scientific, Germany) and incubated at standard conditions in 1 ml cell medium allowed to adhere overnight. Thereafter, the cell medium was removed and replaced by a cell medium containing the released drugs and prepared as previously described. Cells were incubated for 24 h. Subsequently, the viability of the cells was evaluated using a WST-1 assay (WST-1, Roche Diagnostics, Germany) [50,51]. Briefly, 100 µl cell proliferation reagent of WST-1 were added to the culture wells and the cells were incubated for 2 h at cell culture conditions. Formazan produced and released by living cells was quantified spectrometrically at 450 nm with a reference wavelength of 650 nm. Culture medium and reagent WST-1 which had not been into contact with cells was used as blank. As control, MG-63 cells with absence of drugs were incubated and cell viability was determined in the same way as described above. Each test group was set in quadruplicates.

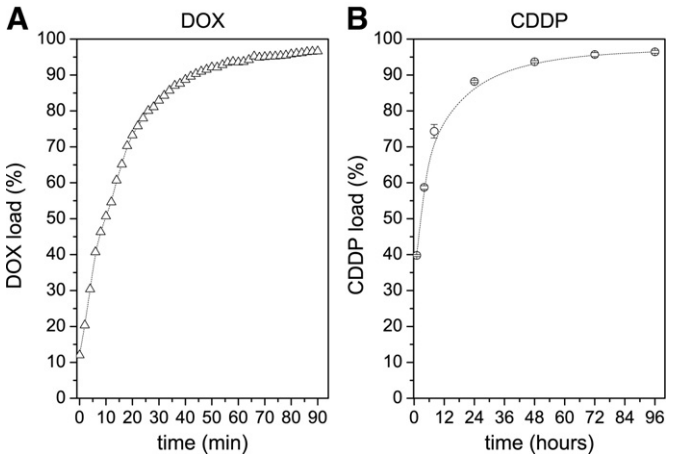

Fig. 4. Doxorubicin (DOX) (A) and cisplatin (CDDP) (B) loading of TCP beads in percent of initial drug concentration (60 µg/ml) versus saturation time. Both drugs were dissolved in ddH_2O.

2.8.4. Statistical analysis

All quantitative data were presented as mean value ± standard deviation. The statistical analysis of the viability test was performed using the statistical software Minitab 17 (Minitab Inc., State College, PA, USA). To investigate the significant differences between the individual sample types, a one-way analysis of variance (ANOVA) with a post hoc Tukey's multiple comparison method was used. p-Values below 0.05 ($p < 0.05$) were considered to be statistically significant.

3. Results

3.1. Bead characterisation

SEM micrographs of non-sintered TCP beads showed roughly spherical geometry with a partially structured, wrinkled, and rough surface

Table 3
Properties of T-ns beads/matrix composites (mean ± SD).

Characteristic	Value
Density ρ (g/cm^3)†	2.68 ± 0.0004
Diameter d (mm)$	14.5 ± 0.03
Height h (mm)$	2.99 ± 0.05
Weight w (g)#	0.77 ± 0.01
Total porosity Φ_t (%)*	60.2 ± 0.95
Open porosity Φ_o (%)§	54.1 ± 4.2
Average pore diameter $d_p^§$	29 nm/16 µm
Pore size distribution§	Bimodal

Measured by: He-pycnometry†, geometrical measurement$, gravimetric measurement#, calculation*, Hg-intrusion§.

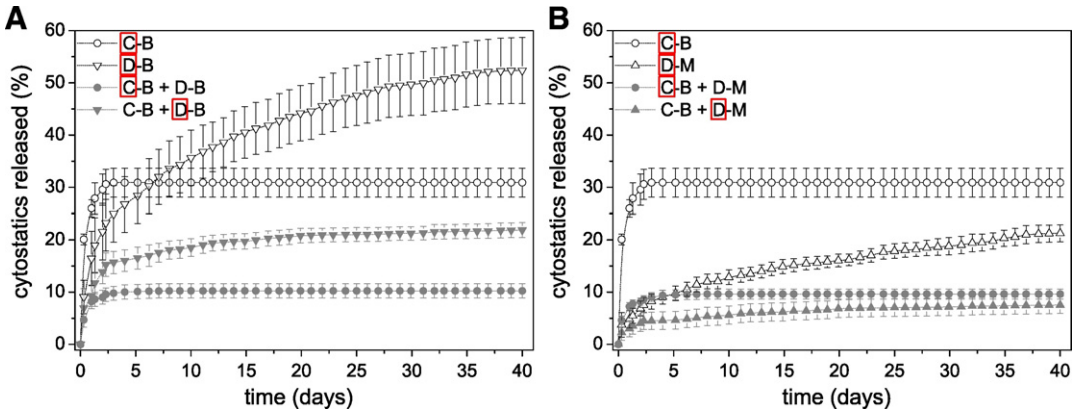

Fig. 5. Cumulative drug release profiles (%) of CDDP from beads (C-B) (A, B), DOX from beads (D-B) (A), respectively DOX from matrix (D-M) (B) in Tris-HCl buffer over 40 d. The amount of released DOX was determined by fluorescence spectrometry ($\lambda_{ex} = 485$ nm; $\lambda_{em} = 590$ nm). CDDP amount was calculated by multi-component analysis using UV/VIS spectrometry and Beer-Lambert law. The red frame indicates the measured drug shown. (mean ± SD).

(Fig. 3). Beads featured a highly porous inner structure encapsulated in a thin, but more compact outer shell as shown by cross section. The densified areas (Fig. 3,C,⋆) are artefacts resulted from sectioning.

Properties of non-sintered TCP beads are summarised in Table 2. Beads had an average diameter of 0.96 mm, density of 2.54 g/cm^3, specific surface area S_{BET} of 55.8 m^2/g, average open porosity of 50.5%, pore volume of 45.5 mm^3/g, and bimodal pore size distribution (average pore diameters at 20 nm and 122 nm).

3.2. Bead drug loading

The loading capability of DOX and CDDP showed great differences in particular with regard to the saturation time (Fig. 4). After 42 min TCP beads were loaded 54 μg/ml of DOX, which corresponded to the ~90% of initial DOX concentration (60 μg/ml). The time required to load the equivalent amount of CDDP was 1.5 days. However, DOX and CDDP showed a comparable loading behaviour. After an initial continuous, nearly linear loading up to ~80%, a considerably slower uptake of the remaining drug amount was observed.

3.3. Composite characteristics

Five different types of beads/matrix composite scaffolds could be prepared by freeze gelation. Cytostatic could be loaded in TCP beads, which could be incorporated in the HAP matrix scaffolds. Moreover, as DOX could be dissolved in water, it could be additionally incorporated in the HAP matrix solution during its fabrication [32–34]. On the contrary, CDDP incorporation in the HAP matrix was not possible, due to its low solubility in aqueous media [35]. Indeed it was possible to dissolve small amounts of CDDP (up to 60 μg/ml) in ddH_2O by shaking, slight heating, or ultrasound to load the beads. However, this was not possible with the ceramic suspension, since these methods would alter the suspension by e.g. bubbles formation or viscosity changes (data not shown).

As shown in Fig. 2,C, TCP beads were homogeneously distributed in the open porous matrix. The beads/matrix scaffolds featured an average density of 2.68 g/cm^3, average total porosity of 60.2%, open porosity of 54.1%, and bimodal pore size distribution with pore sizes of ~29 nm and ~16 μm (Table 3).

3.4. Composite drug release

A different drug release behaviour for the both cytostatics either loaded in beads (CDDP or DOX) or in the matrix structure (DOX) were seen (Fig. 5). Beads/matrix composite scaffolds with CDDP loaded beads showed a sharp and fast burst release of ~30% during the first 3 days of exposure. In contrast, for samples with DOX loaded beads, after a fast initial release of ~20%, a moderate and continuous release followed (Fig. 5,A). During the investigation time of 40 days ~52% of the DOX loaded in beads was released. However, for composites

Table 4
Release kinetic parameters calculated from the drug release data in Tris-HCl buffer using different mathematical models describing drug release mechanisms (R^2 = correlation coefficient; n = diffusional release exponent representing the type of transport; red frame = measured drug).

Formulation	Period (days)	Zero–order kinetic	First–order kinetic	Higuchi's model	Korsmeyer–Peppas model	
		R^2	R^2	R^2	R^2	n
C–B	3	0.1562	0.8571	0.9420	0.9842	0.1921
D–B	40	0.8750	0.9256	0.9746	0.9889	0.3270
C–B + D–B	12	0.4366	0.6838	0.6042	0.7524	0.1651
C–B + D–B	40	0.6629	0.4431	0.8274	0.9150	0.1974
D–M	40	0.9274	0.9411	0.9935	0.9955	0.3724
C–B + D–M	8	0.7464	0.8350	0.7916	0.8973	0.2044
C–B + D–M	40	0.8299	0.6355	0.9470	0.9828	0.2355

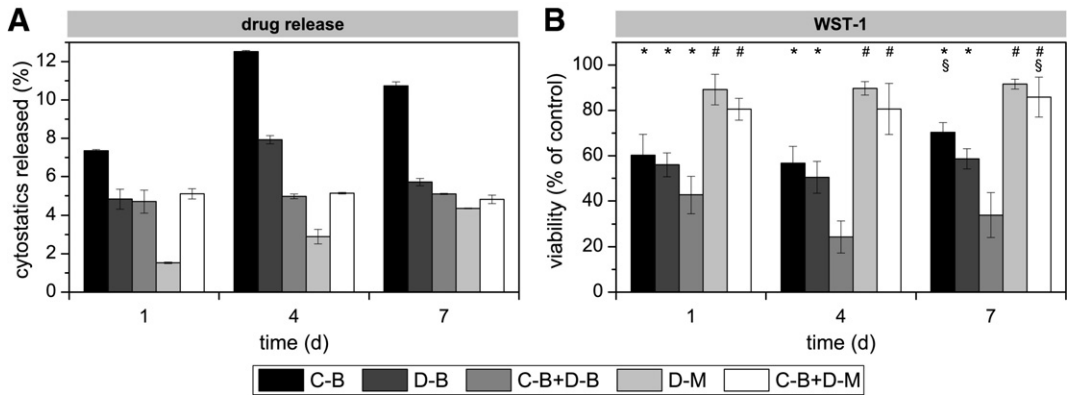

Fig. 6. Drug released (%) (A, C) and resulting viability (% of control) (B, D) of beads/matrix composites after 1, 4, and 7 days drug release in Tris-HCl buffer without medium change. Viability of MG-63 cells on release test supernatants in cell medium (1:9) after 24 h incubation was measured by WST-1 assay. In (B), mean values at one time point that share a symbol (*/#/§) are insignificantly different (ANOVA: Tukey's Multiple Comparison Test, $p < 0.05$).

containing CDDP and DOX loaded beads, a similar release behaviour with a lower amount of each drug released could be observed (Fig. 5,A). CDDP had a sharp burst release until around day 3. The following 9 days only a small amount of CDDP was released (up to ~10% in total) and afterwards the CDDP amount was no longer detectable. DOX showed a faster release within 55 h, followed by a continuous but slowed release. After 40 days 22% of initially contained DOX was released. For composites with CDDP loaded beads and DOX incorporated in the matrix a reduced burst release of DOX could be seen (Fig. 5,B). Overall, with ~21% also a minor amount was released after 40 days compared to composites where DOX was loaded in beads. A combination of CDDP loaded beads and DOX incorporated in the matrix led to a total drug release of ~17%. Thereby, about 10% CDDP until day 8 and 8% DOX until day 40 was released.

The release kinetics for all formulations based on the in vitro release analysis are presented in Table 4. The highest values for the correlation coefficient indicated that all formulations followed Korsmeyer-Peppas release kinetic model [41–43]. Moreover, the diffusional release exponents were found to be between 0.1651 (for CDDP from C-B + D-B) and 0.3724 (for DOX from D-M) and recommended therefore for all composite types and drugs Fickian diffusion.

3.5. Cell viability

Fig. 6 shows the MG-63 cell viability (Fig. 6,B) and cytostatics release without medium change after 1, 4, or 7 days (Fig. 6,A). Samples with CDDP loaded beads (C-B) showed the highest overall release with a maximum of ~13% after 4 days. Samples containing loaded beads with both drugs (C-B + D-B) showed a lower release (~5%) than samples with only one drug type (~8% for DOX (D-B) and ~13% for CDDP (C-B)), especially after day 4. Samples with DOX loaded in matrix (D-M) had the lowest release of only ~4% after day 7. For composites with CDDP loaded beads and DOX in matrix (C-B + D-M) total released drug amounts (~5%) between those with only CDDP loaded beads (C-B) or only DOX loaded matrix (D-M) could be determined.

However, although composites with the CDDP loaded beads (C-B) released highest drug amount, these composites showed not the lowest cell viability (~70% after day 7), thus the toxicity was not the highest. Composites with two different cytostatics loaded in beads (C-B + D-B) had clearly the lowest cell viability (~34%) and thus the highest toxicity with regard to all sample types tested. Samples with DOX in matrix (D-M) showed only a slight decrease in cell viability of ~9%. Composites with both CDDP loaded beads and DOX in matrix (C-B + D-M) had a viability (~81%) that was between the individual samples (C-B and D-M). As reference non-loaded beads/matrix composites were used. At day 1 the reference samples showed a viability of 99.82 ± 9.51% compared to non-treated MG-63 cells, at day 4 a viability of 100.15 ± 4.03%, and at day 7 a viability of 98.45 ± 3.13%. ANOVA analysis with post hoc Tukey's test indicated that samples with one (C-B, D-B) or two (C-B + D-B) cytostatics loaded beads led to statistically significant higher toxicity ($p < 0.05$) compared to composites with loaded matrix (D-M and C-B + D-M). Composites with beads loaded with both drugs (C-B + D-B) lead to a significant higher toxicity at day 4 and day 7 compared to samples with only one drug (C-B and D-B).

4. Discussion

The co-delivery of two different anticancer drugs, namely CDDP and DOX, from calcium phosphate beads/matrix scaffolds could be successfully accomplished and the toxic activity of both released drugs on osteosarcoma cells could be proven. Additionally, by using co-loaded composites a synergistic effect of both cytostatics on toxicity with reduced released drug amount could be determined.

As part of this work, TCP beads were successfully prepared by droplet extrusion with ionotropic gelation. The rough surface and the outer shell of the beads might be caused by TCP dissolution during gelation and inhomogeneous gelation [52,53]. Release of Ca^{2+} ions from TCP might occupy the binding sites of alginate leading to faster cross-linking [28,29,54]. Freezing and drying of the beads leaded to an open porosity of ~51% allowing a good accessibility for the drugs during loading. Pore sizes of non-sintered TCP beads (with averages of 20 nm and 122 nm) are sufficiently large to permit the diffusion of small molecules with sizes of few nanometres like CDDP [55].

The incorporation of ceramic beads in a HAP matrix structure by freeze gelation was proven to be possible without formation of structural defects e.g. large cracks. With this method also complex and individual customisable shapes are feasible [32,33] since the composite should not only be drug carrier but also a scaffold to enable new bone ingrowth. Additionally, incorporation may also prevent an uncontrolled and undesired spreading and migration of the drug carrier in surrounding tissues.

All materials used for preparation consisted of non-toxic substances to guarantee a controlled toxicity by only the cytostatics. As main material CaP were chosen due to the resemblance to natural bone [14,15]. For beads and composite no sintering is required for their mechanical and chemical stability. It is known that CaP shows enhanced degradation when it is not sintered [53]. TCP and HAP were used for beads and matrix, respectively, due to their different dissolution behaviour [53] and that the beads may dissolve much faster. As a result even more and larger pores may be left to achieve an even better bone ingrowth and supply. If beads/matrix composites might degrade with time a complete replacement by healthy natural bone may occur and another surgery to remove the implanted material could be omitted.

Drug loading showed distinct differences in saturation time. Beads loaded DOX ~50 times faster than the same amount CDDP. However, this does not affect the overall homogeneous loading behaviour. For drug loading and release different aqueous media were assayed as their composition can affect drug binding and release. For instance, chloride ions can inhibit CDDP binding, whereas chloride ions are required for its desorption [35]. The loading and release of DOX was carried out in the same media such as CDDP since similar preferences could be detected (see Supplementary data: Fig. A.1). DOX showed faster and enhanced loading in ddH_2O and increased release in Tris-HCl buffer. This can be related to the presence of carboxyl groups of alginate molecules, which can bind to DOX amine groups [56,57]. Additionally, DOX may also bind weakly on TCP surfaces [58]. The adsorption of CDDP to TCP can be explained in terms of electrostatic interactions as result of CDDP hydrolysis in aqueous solutions [35]. Chloride ions are replaced by water molecules creating positively charged species which may bind to the net-negatively charged TCP surface. However, chloride ions in the release medium will reverse the hydrolysis of CDDP which in turn will prevent the adsorption of CDDP on TCP again [59]. As most anticancer drugs, DOX and CDDP also are hydrophobic and can have a limited solubility in aqueous solutions [35,60]. However, DOX in comparison to CDDP is more soluble in water, and therefore it could be dissolved and incorporated in the matrix suspension.

The entire composite can be flowed through and thus the loaded drugs can be released due to the open porous structure and sufficiently large pores of both beads and matrix, respectively. It could be observed a distinct release behaviour according to the cytostatic used, whether only one or in combination, and whether if loaded in the beads or in the matrix. A burst release was observed for CDDP release during the first 3 days by flushing the not bonded drug amount out of the pores. Afterwards, the reversible hydration of the bonded CDDP in presence of the chloride ions in Tris-HCl release medium was gaining importance. However, DOX showed a longer release compared to CDDP, independently if loaded in beads or matrix, respectively. When matrix was loaded with DOX a markedly reduced release of ~30% was observed compared to beads loaded samples. Multi-loaded composites showed a considerably reduced release of both drugs, independently whether DOX were loaded in beads or matrix.

However, the analysis of the release kinetics of all samples indicated that cytostatic release both from beads and matrix followed Korsmeyer-Peppas model. Originally this model was used for polymeric release systems but meanwhile it is often applied and proven to be useful also for porous ceramic delivery systems [42]. Diffusional release exponents revealed for all samples Fickian diffusion, which typically occurs by a chemical potential gradient resulting in molecular diffusion. However, incorporation of DOX into the matrix structure is expected to lead to a hindrance in accessibility, building a drug depot which may release the trapped drug while gradually degradation of the matrix resulting to the observation that the amount of released DOX from the matrix structure was reduced and slowed by ~2.5 times compared when DOX were loaded in beads.

To prove the initial toxicity of released CDDP and DOX from the different loaded beads/matrix composites WST-1 assay was successfully conducted on osteosarcoma cells. This viability test indicated that DOX seemed to have a slightly higher toxicity than CDDP, although the amount of released CDDP in the investigation time period was markedly increased. A substantial impact on the measured toxicity was also observed whether beads or matrix were loaded. DOX loaded beads had a significant more marked effect on MG-63 (dead rate ~40–50%) in comparison to DOX loaded matrix (dead rate ~10%). This suggests that the incorporation of drug loaded beads can increase toxicity and anticancer efficiency. When both cytostatics were incorporated together in one composite a synergistic toxicity enhancement of up to ~75% is observable, although a reduced drug release in comparison to single-loaded samples. Using co-loaded beads/matrix composites is more effective since with reduced released drug concentrations they leaded to increased activity in agreement with the literature [8,23,25,27,60]. It may be expected that the investigated co-loaded beads/matrix composites can enhance and positively affect cytotoxicity while it should reduce undesired systemic side effects during osteosarcoma therapy.

5. Conclusion

The results of this study confirmed that calcium phosphate beads/matrix composites are promising as drug carrier for a potential osteosarcoma therapy by co-delivering the cytostatics CDDP and DOX. Freeze gelation process was shown to be suitable to incorporate drug loaded TCP/alginate beads in an open-porous matrix structure to prevent the drugs from uncontrolled spreading and migration in the surrounding tissue and to act additionally as a scaffold for new bone formation. Also the matrix can be loaded with DOX, which decreases drug release (~22% in 40 days) as compared to a release from DOX loaded beads (~52% in 40 days). However, DOX has a longer diffusion controlled release over 40 days compared to CDDP with only 3 days, independently if loaded in beads or matrix. Co-loaded beads/matrix composites synergistically enhance toxicity towards MG-63 osteosarcoma cells (viability of ~34%) while reducing released drug quantity (~5%) compared to single-loaded composites (~59% viability with ~6% drug release for DOX loaded beads and ~70% viability with ~11% drug release for CDDP loaded beads). The results suggest that our approach of co-loaded ceramic beads/matrix scaffolds can lead to a long-term cytostatic release and synergistic effects of CDDP and DOX and are thereby highly suitable for osteosarcoma therapy.

Supplementary data to this article can be found online at http://dx.doi.org/10.1016/j.msec.2017.03.164.

Acknowledgments

We kindly acknowledge Tina Kuehn for her support with the mercury intrusion and Petra Luecke for her support with the SEM images. This study was partially funded by the ERC starting grant BiocerEng project number 205509.

References

[1] N.G. Sanerkin, Malignancy, aggressiveness, and recurrence in giant cell tumor of bone, Cancer 46 (1980) 1641–1649.
[2] L. Adamsen, M. Quist, C. Andersen, T. Moller, J. Herrstedt, D. Kronborg, M.T. Baadsgaard, K. Vistisen, J. Midtgaard, B. Christiansen, M. Stage, M.T. Kronborg, M. Rorth, Effect of a multimodal high intensity exercise intervention in cancer patients undergoing chemotherapy: randomised controlled trial, BMJ 339 (2009) b3410.
[3] M.R. DiCaprio, G.E. Friedlaender, Malignant bone tumors: limb sparing versus amputation, J. Am. Acad. Orthop. Surg. 11 (2003) 25–37.
[4] J. Livage, T. Coradin, C. Roux, Encapsulation of biomolecules in silica gels, J. Phys. Condens. Matter 13 (2001) R673–R691.
[5] M. Hamidi, A. Azadi, P. Rafiei, Hydrogel nanoparticles in drug delivery, Adv. Drug Deliv. Rev. 60 (2008) 1638–1649.
[6] Y. Mizushima, T. Ikoma, J. Tanaka, K. Hoshi, T. Ishihara, Y. Ogawa, A. Ueno, Injectable porous hydroxyapatite microparticles as a new carrier for protein and lipophilic drugs, J. Control. Release 110 (2006) 260–265.
[7] L. Wu, J. Zhang, W. Watanabe, Physical and chemical stability of drug nanoparticles, Adv. Drug Deliv. Rev. 63 (2011) 456–469.
[8] S.M. Lee, T.V. O'Halloran, S.T. Nguyen, Polymer-caged nanobins for synergistic cisplatin-doxorubicin combination chemotherapy, J. Am. Chem. Soc. 132 (2010) 17130–17138.
[9] X. Sun, J. Shi, X. Xu, S. Cao, Chitosan coated alginate/poly(*N*-isopropylacrylamide) beads for dual responsive drug delivery, Int. J. Biol. Macromol. 59 (2013) 273–281.
[10] Z. Liu, Y. Jiao, Y. Wang, C. Zhou, Z. Zhang, Polysaccharides-based nanoparticles as drug delivery systems, Adv. Drug Deliv. Rev. 60 (2008) 1650–1662.
[11] E. Verron, I. Khairoun, J. Guicheux, J.-M. Bouler, Calcium phosphate biomaterials as bone drug delivery systems: a review, Drug Discov. Today 15 (2010) 547–552.
[12] A. Barroug, L.T. Kuhn, L.C. Gerstenfeld, M.J. Glimcher, Interactions of cisplatin with calcium phosphate nanoparticles: in vitro controlled adsorption and release, J. Orthop. Res. 22 (2004) 703–708.
[13] G. Spenlehauer, M. Vert, J.P. Benoit, A. Boddaer, In vitro and in vivo degradation of poly(D,L lactide/glycolide) type microspheres made by solvent evaporation method, Biomaterials 10 (1989) 557–563.

[14] D. Arcos, M. Vallet-Regi, Bioceramics for drug delivery, Acta Mater. 61 (2013) 890–911.
[15] W.J.E.M. Habraken, J.G.C. Wolke, J.A. Jansen, Ceramic composites as matrices and scaffolds for drug delivery in tissue engineering, Adv. Drug Deliv. Rev. 59 (2007) 234–248.
[16] X. Cheng, L. Kuhn, Chemotherapy drug delivery from calcium phosphate nanoparticles, Int. J. Nanomedicine 2 (2007) 667–674.
[17] S. Dasari, P.B. Tchounwou, Cisplatin in cancer therapy: molecular mechanisms of action, Eur. J. Pharmacol. 740 (2014) 364–378.
[18] A.M. Florea, D. Büsselberg, Cisplatin as an anti-tumor drug: cellular mechanisms of activity, drug resistance and induced side effects, Cancer 3 (2011) 1351–1371.
[19] O. Tacar, P. Sriamornsak, C.R. Dass, Doxorubicin: an update on anticancer molecular action, toxicity and novel drug delivery systems, J. Pharm. Pharmacol. 65 (2013) 157–170.
[20] A.C. Jayasuriya, A.J. Darr, Controlled release of cisplatin and cancer cell apoptosis with cisplatin encapsulated poly(lactic-*co*-glycolic acid) nanoparticles, J. Biomed. Sci. Eng. 6 (2013) 586–592.
[21] D.W. Shen, L.M. Pouliot, M.D. Hall, M.M. Gottesman, Cisplatin resistance: a cellular self-defense mechanism resulting from multiple epigenetic and genetic changes, Pharmacol. Rev. 64 (2012) 706–721.
[22] M. Biondi, S. Fusco, A.L. Lewis, P.A. Netti, Investigation of the mechanisms governing doxorubicin and irinotecan release from drug-eluting beads: mathematical modeling and experimental verification, J. Mater. Sci. Mater. Med. 24 (2013) 2359–2370.
[23] J. Lehàr, A.S. Krueger, W. Avery, A.M. Heilbut, L.M. Johansen, E.R. Price, R.J. Rickles, G.F. Short III, J.E. Staunton, X. Jin, M.S. Lee, G.R. Zimmermann, A.A. Borisy, Synergistic drug combinations improve therapeutic selectivity, Nat. Biotechnol. 27 (2009) 659–666.
[24] J.T. Thigpen, M.F. Brady, H.D. Homesley, J. Malfetano, B. DuBeshter, R.A. Burger, S. Liao, Phase III trial of doxorubicin with or without cisplatin in advanced endometrial carcinoma: a gynecologic oncology group study, J. Clin. Oncol. 22 (2004) 3902–3908.
[25] L. Cai, G. Xu, C. Shi, D. Guo, X. Wang, J. Luo, Telodendrimer nanocarrier for co-delivery of paclitaxel and cisplatin: a synergistic combination nanotherapy for ovarian cancer treatment, Biomaterials 37 (2015) 456–468.
[26] V. Shanmugam, Y.H. Chien, Y.S. Cheng, T.Y. Liu, C.C. Huang, C.H. Su, Y.S. Chen, U. Kumar, H.F. Hsu, C.S. Yeh, Oligonucleotides-assembled Au nanorod-assisted cancer photothermal ablation and combination chemotherapy with targeted dual-drug delivery of doxorubicin and cisplatin prodrug, ACS Appl. Mater. Interfaces 6 (2014) 4382–4393.
[27] M. Li, Z. Tang, S. Lv, W. Song, H. Hong, X. Jing, Y. Zhang, X. Chen, Cisplatin crosslinked pH-sensitive nanoparticles for efficient delivery of doxorubicin, Biomaterials 35 (2014) 3851–3864.
[28] T.Y. Klein, L. Treccani, K. Rezwan, Ceramic microbeads as adsorbents for purification technologies with high specific surface area, adjustable pore size, and morphology obtained by ionotropic gelation, J. Am. Ceram. Soc. 95 (2012) 907–914.
[29] A. Blandino, M. Macias, D. Cantero, Formation of calcium alginate gel capsules: influence of sodium alginate and CaCl2 concentration on gelation kinetics, J. Biosci. Bioeng. 88 (1999) 686–689.
[30] B. Anilanmert, G. Yalçin, F. Ariöz, E. Dölen, The spectrometric determination of cisplatin in urine, using o-phenylenediamine as derivatizing agent, Anal. Lett. 34 (2001) 113–123.
[31] M. Basotra, S.K. Singh, M. Gulati, Development and validation of a simple and sensitive spectrometric method for estimation of cisplatin hydrochloride in tablet dosage forms: application to dissolution studies, ISRN Anal. Chem. (2013) 1–8.
[32] U. Hess, S. Hill, L. Treccani, P. Streckbein, C. Heiss, K. Rezwan, A mild one-pot process for synthesising hydroxyapatite/biomolecule bone scaffolds for sustained and controlled antibiotic release, Biomed. Mater. 10 (2015) 015013.
[33] U. Hess, G. Mikolajczyk, L. Treccani, P. Streckbein, C. Heiss, S. Odenbach, K. Rezwan, Multi-loaded ceramic beads/matrix scaffolds obtained by combining ionotropic and freeze gelation for sustained and tuneable vancomycin release, Mater. Sci. Eng. C 67 (2016) 542–553.
[34] B. Mueller, D. Koch, R. Lutz, K.A. Schlegel, L. Treccani, K. Rezwan, A novel one-pot process for near-net-shape fabrication of open-porous resorbable hydroxyapatite/protein composites and in vivo assessment, Mater. Sci. Eng. C 42 (2014) 137–145.
[35] A. Barroug, M.J. Glimcher, Hydroxyapatite crystals as a local delivery system for cisplatin: adsorption and release of cisplatin in vitro, J. Orthop. Res. 30 (2002) 274–280.
[36] S. Brunauer, P.H. Emmett, E. Teller, Adsorption of gases in multimoleculer layers, J. Am. Ceram. Soc. 60 (1938) 309–319.
[37] S. Othman, Multicomponent derivative spectroscopic analysis of sulfamethoxazole and trimethoprim, Int. J. Pharm. 63 (1990) 173–176.
[38] S. Sahoo, C.K. Chakraborti, P.K. Behera, Development and evaluation of gastroretentive controlled release polymeric suspensions containing ciprofloxacin and carbopol polymers, J. Chem. Pharm. Res. 4 (2012) 2268–2284.
[39] G. Yadav, M. Bansal, N. Thakur, S. Khare, P. Khare, Multilayer tablets and their drug release kinetic models for oral controlled drug delivery system, Middle-East J. Sci. Res. 16 (2013) 782–795.
[40] P. Costa, J.M. Sousa Lobo, Modeling and comparison of dissolution profiles, Eur. J. Pharm. Sci. 13 (2001) 123–133.
[41] G. Singhvi, M. Singh, In-vitro drug release characterization models, IJPSR 2 (2011) 77–84.
[42] U. Gbureck, E. Vorndran, J.E. Barralet, Modeling vancomycin release kinetics from microporous calcium phosphate ceramics comparing static and dynamic immersion conditions, Acta Biomater. 4 (2008) 1480–1486.
[43] J. Siepmann, N.A. Peppas, Modeling of drug release from delivery systems based on hydroxypropyl methylcellulose (HPMC), Adv. Drug Deliv. Rev. 48 (2001) 139–157.
[44] S. Shahabi, L. Treccani, R. Dringen, K. Rezwan, Dual fluorophore doped silica nanoparticles for cellular localization studies in multiple stained cells, Acta Biomater. 14 (2015) 208–216.
[45] S. Shahabi, L. Treccani, K. Rezwan, Amino acid-catalyzed seed regrowth synthesis of photostable high fluorescent silica nanoparticles with tunable sizes for intracellular studies, J. Nanopart. Res. 17 (2015) 1–15.
[46] S. Shahabi, L. Treccani, R. Dringen, K. Rezwan, Modulation of silica nanoparticle uptake into human osteoblast cells by variation of the ratio of amino and sulfonate surface groups: effects of serum, ACS Appl. Mater. Interfaces 7 (2015) 13821–13833.
[47] S. Shahabi, L. Treccani, R. Dringen, K. Rezwan, Utilizing the protein corona around silica nanoparticles for dual drug loading and release, Nanoscale 7 (2015) 16251–16265.
[48] DIN EN ISO 10993-5, Biological Evaluation of Medical Devices - Part 5: Tests for In Vitro Cytotoxicity (German version), 2009.
[49] F. Chai, M. Abdelkarim, T. Laurent, N. Tabary, S. Degoutin, N. Simon, F. Peters, N. Blanchemain, B. Martel, H.F. Hildebrand, Poly-cyclodextrin functionalized porous bioceramics for local chemotherapy and anticancer bone reconstruction, J. Biomed. Mater. Res. B Appl. Biomater. 102 (2014) 1130–1139.
[50] M. Große Holthaus, L. Treccani, K. Rezwan, Osteoblast viability on hydroxyapatite with well-adjusted submicron and micron surface roughness as monitored by the proliferation reagent WST-1, J. Biomater. Appl. 27 (2012) 791–800.
[51] K. Pardun, L. Treccani, E. Volkmann, P. Streckbein, C. Heiss, G. Li Destri, G. Marletta, K. Rezwan, Mixed zirconia calcium phosphate coatings for dental implants: tailoring coating stability and bioactivity potential, Mater. Sci. Eng. C 48 (2015) 337–346.
[52] C.P. Klein, J.M. de Blieck-Hogervorst, J.G. Wolke, K. de Groot, Studies of the solubility of different calcium phosphate ceramic particles in vitro, Biomaterials 11 (1990) 509–512.
[53] R.Z. LeGeros, Biodegradation and bioresorption of calcium phosphate ceramics, Clin. Mater. 14 (1993) 65–88.
[54] K. Potter, B.J. Balcom, T.A. Carpenter, L.D. Hall, The gelation of sodium alginate with calcium ions studied by magnetic resonance imaging (MRI), Carbohydr. Res. 257 (1994) 117–126.
[55] T. Boulikas, Molecular mechanisms of cisplatin and its liposomally encapsulated form, Lipoplatin™. Lipoplatin™ as a chemotherapy and antiangiogenesis drug, Cancer Ther. 5 (2007) 351–376.
[56] C. Yang, J.P. Tan, W. Cheng, A.B. Attia, C. Tan Yi Ting, A. Nelson, J.L. Hedrick, Y.-Y. Yang, Supramolecular nanostructures designed for high cargo loading capacity and kinetic stability, Nano Today 5 (2010) 515–523.
[57] A.B. Attia, C. Yang, J.P. Tan, S. Gao, D.F. Williams, J.L. Hedrick, Y.Y. Yang, The effect of kinetic stability on biodistribution and anti-tumor efficacy of drug-loaded biodegradable polymeric micelles, Biomaterials 34 (2013) 3132–3140.
[58] R.J. Sturgeon, C. Flanagan, D.V. Naik, S.G. Schulman, In vitro adsorption of doxorubicin hydrochloride on insoluble calcium phosphate, J. Pharm. Sci. 66 (1977) 1346–1347.
[59] B. Palazzo, M. Iafisco, M. Laforgia, N. Margiotta, G. Natile, C.L. Bianchi, D. Walsh, S. Mann, N. Roveri, Biomimetic hydroxyapatite–drug nanocrystals as potential bone substitutes with antitumor drug delivery properties, Adv. Funct. Mater. 17 (2007) 2180–2188.
[60] W. Zhu, Y. Li, L. Liu, Y. Chen, F. Xi, Supramolecular hydrogels as a universal scaffold for stepwise delivering Dox and Dox/cisplatin loaded block copolymer micelles, Int. J. Pharm. 437 (2012) 11–19.